Transition-Metal-Promoted C−N Bond-Formation Processes − Low-Spin Fe^{III}, Fe^{II}, and Ni^{II} Complexes of 2-[(Arylamido)phenylazo]pyridine − X-ray Structure, Redox- and Spectroelectrochemistry

Amrita Saha,[a] Partha Majumdar,[a] Shie-Ming Peng,[b] and Sreebrata Goswami*[a]

Dedicated to Professor Animesh Chakravorty on the occasion of his 65th birthday

Keywords: Transition-metal-promoted reactions / Aminations / Iron / Nickel / Electrochemistry / N ligands

The metal-promoted amination of an aromatic ring of coordinated L^1 [L^1, pap = 2-(phenylazo)pyridine] is described. Whereas the labile cobalt complex $[Co(L^1)_3]^{2+}$ prefers *ortho*-amination, yielding L^2H {2-[2-(arylamino)phenylazo]-pyridine}, the corresponding $[Fe(L^1)_3]^{2+}$ complex produces the *para*-aminated product L^3H {2-[4-(arylamino)-phenylazo]pyridine}. Both L^2H and L^3H have been isolated in the pure state and were fully characterised. They have low pK_a values, for example pK_a(L^{2a}H) = 8.5 ± 1 and pK_a(L^{3a}H) = 9.1 ± 1. Upon deprotonation, the ligand L^2H behaves as a potential tridentate N,N,N donor. It reacts with anhydrous $FeCl_3$ and $NiCl_2{\cdot}6H_2O$ to produce cationic $[Fe(L^2)_2]^+$ (**1**$^+$) and neutral $[Ni(L^2)_2]$ (**2**), respectively. The cationic ferric complex has been isolated as its perchlorate salt, which is paramagnetic with one unpaired electron (1.66 μ_B). It shows a rhombic EPR spectrum with g_1 = 2.11, g_2 = 2.08, g_3 = 1.93. The room-temperature magnetic moment of the nickel complex is 2.89 μ_B, which confirms the presence of two unpaired electrons. The representative X-ray structures of [**1**]ClO_4 and **2** are reported. In both cases the azo nitrogen atoms of the coordinated ligand, $[L^2]^-$ approach the metal centres more closely, and there is a significant degree of ligand backbone conjugation. The complexes display multiple redox responses. Chemical reduction of **1**$^+$ with dilute hydrazine affords the corresponding ferrous complex $[Fe(L^2)_2]$ (**1**) in almost quantitative yield. The spectral changes upon electrolysis of the above couples have been recorded in an OTTLE cell.

Introduction

Reactions of coordinated ligands belong to an important class of chemical transformations,[1−5] as they provide facile synthetic routes for the formation of many novel molecules that are otherwise difficult, or even impossible, to synthesise by conventional synthetic procedures. We are interested in the aromatic ring amination of coordinated azoarene ligands. In this respect, we have recently described[6,7] cobalt- and rhodium-promoted amination processes of the coordinated 2-(phenylazo)pyridine ligand (pap, L^1). Upon coordination, the phenyl ring of the ligand L^1 is activated, and as a result, both *ortho*- and *para*-amination processes were observed (Scheme 1). The *ortho*-aminated product L^2H can act as a monoanionic tridentate N,N,N donor with the dissociation of the amine proton.

The *para*-aminated product L^3H, on the other hand, binds as a neutral bidentate N,N-donor.[6] The tridentate ligand $[L^2]^-$ has a unique combination of hard as well as soft donor sites. The strong acceptor ability of the azopyridine moiety[8] is capable of stabilising low oxidation states of the metal centre, while the strong electron donor

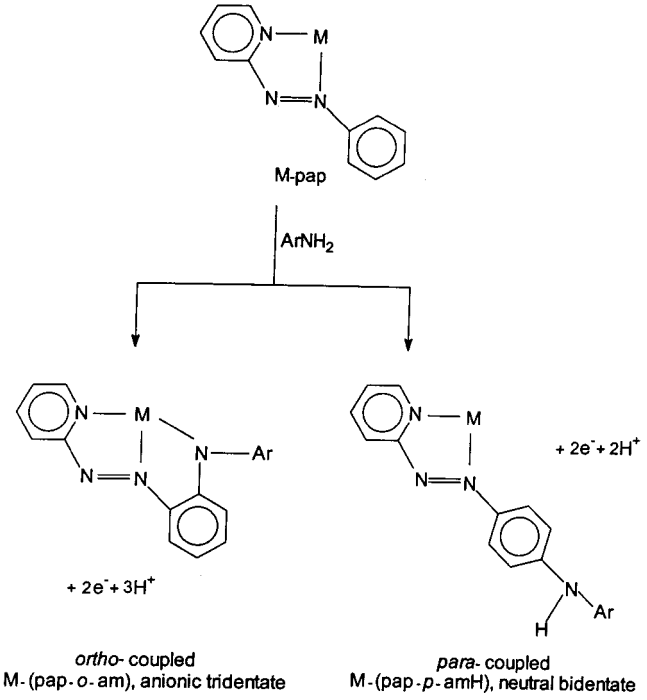

Scheme 1. Amination of the coordinated ligand 2-(phenylazo)pyridine

[a] Department of Inorganic Chemistry, Indian Association for the Cultivation of Science,
Calcutta 700032, India
Fax: (internat.) + 91-33/473-2805
E-mail: icsg@mahendra.iacs.res.in
[b] Department of Chemistry, National Taiwan University,
Taipei, Taiwan, Republic of China
Supporting information for this article is available on the WWW under http://www.wiley-vch.de/home/eurjic or from the author.

  1434−1948/00/1212−2631 $ 17.50+.50/0

amido part is expected to stabilise the high-valent metal centre. Thus, tunable donor-acceptor properties of this ligand that depend on the oxidation state of the metal centre may be found. It should be noted here that the anionic ligand $[L^2]^-$ reacts readily with the respective metal salts to produce[9] octahedral low-spin complexes of Mn^{II} and Co^{III}.

Two interrelated aspects, viz. metal-promoted reactions of the coordinated azopyridine ligand and the coordination chemistry thereof, are of great interest in this area. As a logical continuation of this project, we report here the first isolation of the *para*-aminated ligand L^3H, together with the coordination chemistry of $[L^2]^-$ involving low-spin Fe^{II} and Fe^{III} ions, and Ni^{II} ion. It may be worth noting that examples of stable and structurally characterised low-spin ferric complexes are rare in the literature.[10–12]

Results and Discussion

Iron- and Nickel-Promoted Aromatic Ring Amination of Coordinated 2-(Phenylazo)pyridine (L^1)

The neutral ligand, L^1 is known to form cationic tris(chelates) of the type $[M(L^1)_3]^{2+}$ (M = Co^{II}, Fe^{II}, and Ni^{II}) with the respective metal ions.[13] The labile cobalt complex $[Co(L^1)_3]^{2+}$ reacts smoothly with primary aromatic amines ($ArNH_2$), without solvent, to produce[6] green, crystalline complexes $[Co^{III}(L^2)_2]^+$. The free ligand $[L^2H]$ has been isolated[9] by the removal of the metal ion from $[Co(L^2)_2]^+$ (Scheme 2). Similarly, the corresponding Fe^{II} and Ni^{II} complexes $[M(L^1)_3]^{2+}$ react with $ArNH_2$ to produce blue or blue-violet mixtures. Unfortunately, these compounds could not be purified. They decompose rapidly in solution and give inconsistent analyses. The blue iron intermediate is diamagnetic, but the nickel compound is paramagnetic. The iron intermediate is thus an Fe^{II} complex. However, the transformed organic ligands can be isolated from these crude mixtures by the removal of the metal ions (Scheme 3).

$$[Co^{II}(L^1)_3]^{2+} \xrightarrow{ArNH_2} [Co^{III}(L^2)_2]^+ \xrightarrow{N_2H_4/(NH_4)_2S_x} [L^2H] + CoS + \text{Other products}$$
Brown Green Orange

Scheme 2. Preparation of the ligand L^2H

$$[Fe^{II}(L^1)_3]^{2+} \xrightarrow{ArNH_2} [\text{Intermediate}] \xrightarrow{\text{aq. } NH_3} [L^3H] + Fe_2O_3.nH_2O + \text{Other products}$$
Blue Deep blue Yellow

$$[Ni^{II}(L^1)_3]^{2+} \xrightarrow{ArNH_2} [\text{Intermediate}] \xrightarrow{(NH_4)_2S_x} [L^2H] + [L^3H] + NiS + \text{Other products}$$
Green Blue-violet Organge Yellow

Scheme 3. Isolation of the ligands L^2H and L^3H

While only *ortho*-amination was observed in the case of $[Co(L^1)_3]^{2+}$, the *para*-aminated ligand L^3H is the only product obtained from $[Fe(L^1)_3]^{2+}$. In contrast, the corresponding nickel compound $[Ni(L^1)_3]^{2+}$ produced a mixture of $[L^2H]$ and $[L^3H]$ in almost equal proportions. The actual reasons for the regioselectivity of these amination processes are yet to be established. It has been shown, however, that prior coordination of the amine residue to the metal centre is an important prerequisite for an *ortho*-amination process of the above type, which is favoured in the case of a labile metal complex.[6] Of the three (pap)metal complexes mentioned above, $[Co(pap)_3]^{2+}$ is kinetically most labile and readily dissociates one pap moiety in solution. These amination reactions are ($2\,e^- + 2\,H^+$) transfer processes and occur in the presence of air, which is the source of the oxidising agent.

Isolation and Characterisation of $[L^3H]$

A methanolic solution of the blue mixture obtained from the reaction of $[Fe(L^1)_3]^{2+}$ and $ArNH_2$ on treatment with NH_3(aq.) precipitated brown hydrated ferric oxide and the solution became yellow. Upon work-up $[L^3H]$ was obtained as orange crystals (Scheme 3). Two such compounds viz. $[L^{3a}H]$ and $[L^{3b}H]$ ($L^{3a}H$: $ArNH_2$ = aniline and $L^{3b}H$: $ArNH_2$ = *p*-toluidine) were isolated. Both the ligands show highly resolved ^1H NMR spectra in $CDCl_3$. The N–H resonance appears as a broad singlet at $\delta = 6.12$. This is in marked contrast to the corresponding *ortho* ligand, where the N–H resonates at $\delta = 10.58$. In the *ortho* isomer, intramolecular hydrogen bonding is expected which is absent in the *para* isomer. For the ^1H NMR spectrum of $[L^{3b}H]$ see Supporting Information. The reagent ammoniacal polysulfide was used to decompose the nickel intermediate.

The ligand $[L^{3a}H]$ formed crystals suitable for a single-crystal X-ray structure determination. The structure confirms the formation of $[L^{3a}H]$ from coordinated L^1 and aniline. The ORTEP and atom numbering scheme are shown in Figure 1. The geometry of this ligand is *trans* about the diazo fragment. The N–N distance is 1.264(2) Å, which is indicative of a double bond. For comparison, this distance[14] in $[L^1H]ClO_4$ is 1.258(5) Å. All other bond lengths are within the range of normally observed values. The pyridyl ring, diazo function, phenyl ring, and amine nitrogen atoms are all coplanar. The terminal phenyl group is out of this plane by ca. 44°. The tetrahedral nature of the amine

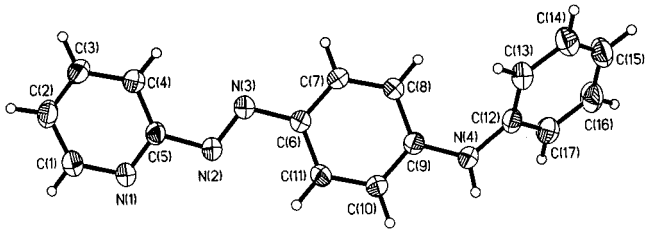

Figure 1. Molecular structure and atom numbering scheme for $[L^{3a}H]$; selected bond lengths [Å]: N(1)–C(5) 1.337(2), N(2)–C(5) 1.427(2), N(2)–N(3) 1.264(2), N(3)–C(6) 1.408(2), C(6)–C(10) 1.394(3), C(10)–C(11) 1.370(2), C(9)–C(10) 1.401(2), N(4)–C(9) 1.383(2), N(4)–C(12) 1.405(2), C(12)–C(13) 1.382(3)

nitrogen atom N(4) may be assessed by the nonplanarity of the two phenyl rings attached to it.

The Iron and Nickel Complexes of $[L^2]^-$

The 1:2 reaction of anhydrous $FeCl_3$ with $[L^2H]$ in methanol in the presence of dilute NEt_3 produced a brown solution at room temperature. Subsequent addition of dilute aqueous $NaClO_4$ afforded crystalline $[Fe(L^2)_2]ClO_4$, [**1**]ClO_4 in excellent yields. The green nickel(II) complexes, $[Ni(L^2)_2]$ (**2**) were obtained directly from the reaction of hydrated nickel(II) chloride with $[L^2H]$ in the presence of dilute NEt_3 (Scheme 4).

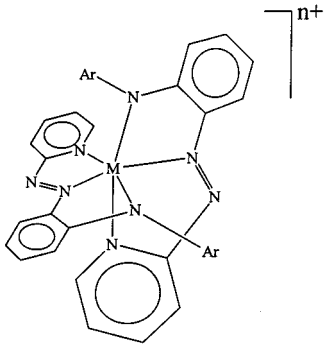

$M = Fe^{III}$; $n = 1$

$M = Ni^{II}$; $n = 0$

Scheme 4. Schematic diagram of the metal complexes, $[M(L^2)_2]^{n+}$

In solution, the bivalent nickel complex behaves as a non-electrolyte, whereas the complex $[Fe(L^2)_2]ClO_4$ is a 1:1 electrolyte[15] (Λ = 135−140 $\Omega^{-1}cm^2M^{-1}$ in MeCN). The room-temperature (298 K) magnetic moments of solid $[Fe(L^2)_2]ClO_4$ and $[Ni(L^2)_2]$ lie in the ranges 1.66−1.73 μ_B and 2.89−2.93 μ_B, respectively. Thus, the iron compound is in a low-spin state, $t_2^5(Fe^{III})$. For comparison, the magnetic moments of the corresponding low-spin manganese(II) complex $[Mn(L^2)_2]$ are observed[9] in the range 1.65−1.70 μ_B. In frozen (77 K) dichloromethane/toluene solution the ferric complexes display rhombic spectra with g_1 = 2.11, g_2 = 2.08, and g_3 = 1.93. The rhombic nature of EPR spectra in the present case indicates the asymmetry of the electronic environment around Fe^{III}. The spectrum may be considered as pseudo-axial, consisting of a rather isolated signal g_3 (g_{II} in the true axial case) and two relatively close signals g_1 and g_2 (rhombic components of $g_\perp$). Accordingly, the axial distortion (Δ) that splits the t_2 levels into a and e components is expected to be larger[16] than the rhombic distortion (V) that splits e. The EPR spectral pattern further confirms[11] the low-spin state of iron in $[Fe(L^2)_2]^+$.

Structures

Figure 2 and Figure 3 show the ORTEP and atom numbering schemes for [**1a**]$^+$ and **2a**, respectively.

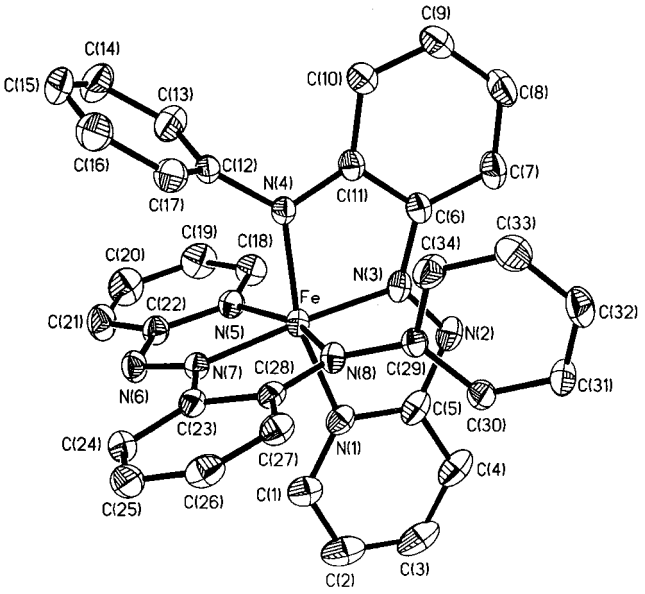

Figure 2. Molecular structure and atom numbering scheme for $[Fe(L^{2a})_2]^+$ cation in $[Fe(L^{2a})_2]$ ClO_4; selected bond lengths [Å]: Fe−N(1) 1.962(2), Fe−N(3) 1.885(2), Fe−N(4) 1.914(2), Fe−N(5) 1.969(2), Fe−N(7) 1.880(2), Fe−N(8) 1.921(2), N(1)−C(5) 1.366(3), N(2)−C(5) 1.379(3), N(2)−N(3) 1.304(2), N(3)−C(6) 1.373(3), C(6)−C(11) 1.425(3), N(4)−C(11) 1.355(3), N(4)−C(12) 1.432(2)

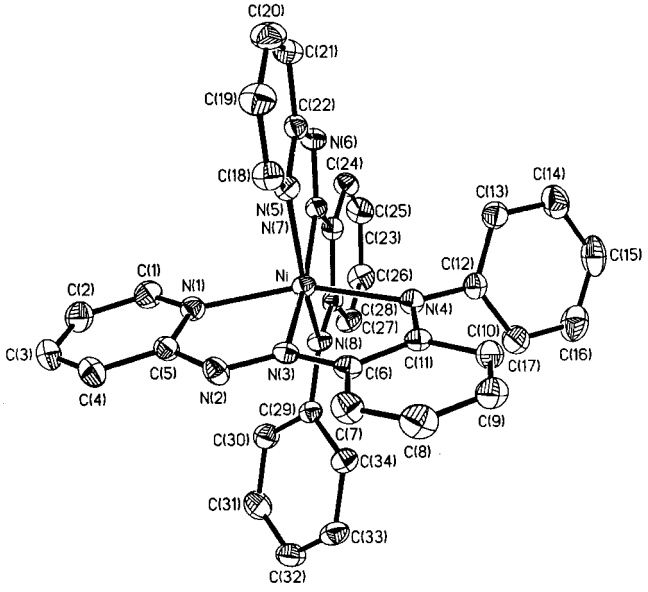

Figure 3. Molecular structure and atom numbering scheme for $[Ni(L^{2a})_2]$; selected bond lengths [Å]: Ni−N(1) 2.099(2), Ni−N(3) 2.002(2), Ni−N(4) 2.079(2), Ni−N(5) 2.103(2), Ni−N(7) 1.989(2), Ni−N(8) 2.078(2), N(1)−C(5) 1.346(3), N(2)−C(5) 1.394(3), N(2)−N(3) 1.301(3), N(3)−C(6) 1.348(3), C(6)−C(11) 1.447(3), N(4)−C(11) 1.318(3), N(4)−C(12) 1.418(3)

The structural analysis of cationic $[Fe(L^{2a})_2]^+$ reveals the presence of two ligands, each of which acts as an N,N,N-tridentate donor with deprotonation of the amine nitrogens, viz. N(4) and N(8). Its geometry is meridional and the Fe atom sits on an imposed C_2 axis bisecting the angles

N(1)−Fe−N(5) and N(4)−Fe−N(8). The two azo nitrogen atoms of the anionic tridentate ligands approach the metal centre more closely [Fe−N(3)/N(7) ≈ 1.88 Å] than the other four Fe−N bonds. There is an indication of significant backbone conjugation in the coordinated anionic ligand. Notably, the N=N azo distances in these complexes are appreciably elongated. For example, this bond length in [**1a**]ClO_4 (1.299 Å) is much longer than in $L^{3a}H$ (1.264 Å). This change is reflected in the reduction of $\nu_{N=N}$ in [**1a**]ClO_4, which appears at 1370 cm^{-1}. In the infrared spectrum of $L^{2a}H$, the $\nu_{N=N}$ stretching is observed at 1420 cm^{-1}. Moreover, the bond length N(azo)−C(phenyl) (1.377 Å) is shorter than the value of 1.421 Å found for the corresponding distance[14] in the salt [Hpap]ClO_4. Similarly, the amido nitrogen atom of $[L^{2a}]^-$ binds to the phenyl group of pap at a shorter distance than is observed for a N−C(phenyl) single bond. These are all in agreement with the notion of extensive electron delocalisation along the ligand backbone. Some degree of conjugation along the ligand backbone of this bis(chelate) system could be implicated in the shortening of Fe−N(azo) bonds, either through an increase in the electron density on N(azo) and a concomitant increased basicity or through an enhanced π-bonding capability of the more conjugated ligand.

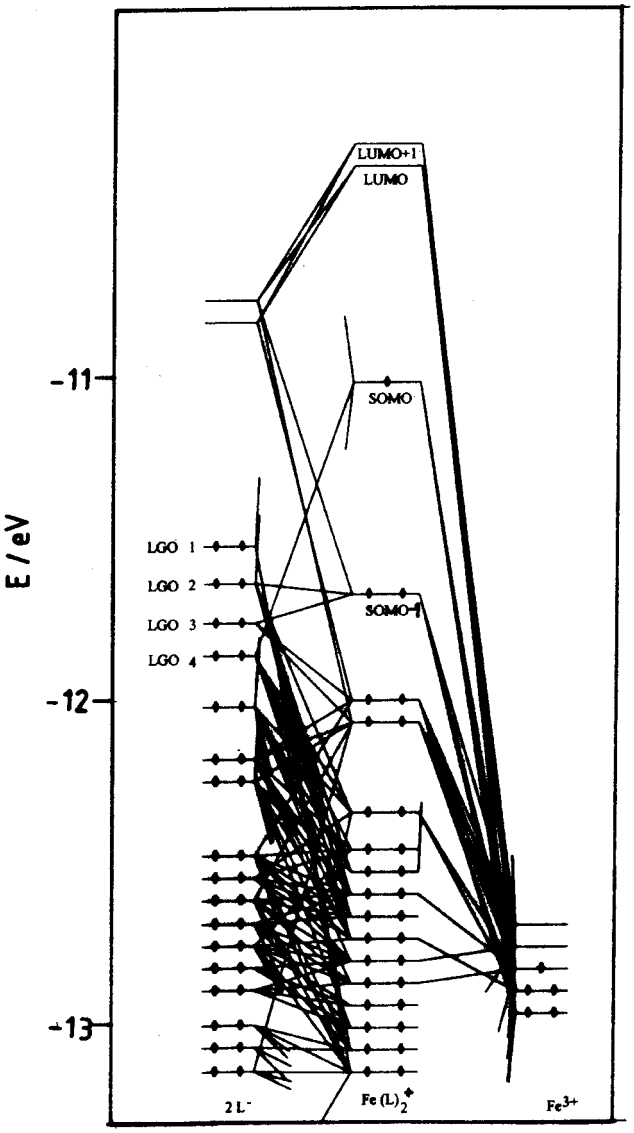

Figure 4. Partial energy level diagram of $[Fe(L^{2a})_2]^+$; for pictorial representations of the ligand group orbitals (LGO) see Supporting Information

The main features of the structure of the molecular complex $[Ni(L^{2a})_2]$ (**2a**) are very similar to those for **1a**$^+$. The two anionic ligands $[L^{2a}]^-$ bind the metal ion in an N_6 fashion using pairs of pyridyl-N, azo-N, and deprotonated arylamido-N atoms. The relative orientations within the pairs are *cis*, *trans*, and *cis*, respectively. The chelate bite angles are dissimilar, and are considerably less than the ideal octahedral value (90°). Extensive electron delocalization along the ligand backbone has also been observed in this case. As a result, the N−N(diazo) distances are longer than the usual N=N distance, and the average of the two Ni−N(azo) distances is shorter than the other Ni−N distances in this molecule.

From the crystallographic data it is obvious that the metal complexes under consideration may best be described as delocalised systems. In order to have some insight into the nature of redox and spectroscopically relevant orbitals, a standard extended Hückel MO calculation using the crystallographic parameters was performed on $[Fe(L^{2a})_2]^+$ using the CACAO programme by Mealli and Proserpio.[17] A partial energy level scheme for $[Fe(L^{2a})_2]^+$ is shown in Figure 4. In this complex the SOMO is strongly delocalised. It has 40% metal d-character with significant contributions from both amide and azo functions. The next lower orbital, SOMO-1, is a ligand orbital where the metal contribution is only 11%. There are two closely spaced LUMO and LUMO+1 orbitals which are predominantly ligand π-acceptor orbitals (−N=N− + phenyl rings) with an admixture of 18−19% metal d-character. For pictorial presentation of the above four MOs see Supporting Information.

Redox Properties and Behaviour

The redox properties of the iron and nickel complexes have been studied by cyclic voltammetry (CV) with a platinum working electrode. Voltammetric data are collected in Table 1 and representative voltammograms are displayed in

Table 1. Cyclic voltammetric data

Compound	Oxidation $E_{1/2}$ [V][a]	Reduction $E_{1/2}$ [V][a]
$[Fe(L^{2a})_2]ClO_4$	1.1, 1.75[b]	0.18, −0.97, −1.45
$[Fe(L^{2b})_2]ClO_4$	1.05, 1.73[b]	0.16, −1.01, −1.49
$[Ni(L^{2a})_2]$	0.56, 0.85[c], 1.48[b]	−1.10, −1.26[d]
$[Ni(L^{2b})_2]$	0.54, 0.84[c], 1.45[b]	−1.13, −1.28[d]
$L^{2a}H$	1.00,[b] 1.30[b]	−1.15

[a] Experiments were carried out in CH_3CN at 298 K using TEAP as supporting electrolyte. The reported data corresponds to a scan rate of 50 mVs^{-1}. − [b] Irreversible anodic response, the potential corresponds to E_{pa}. − [c] $i_{pa} > i_{pc}$. − [d] Irreversible cathodic response, the potential corresponds to E_{pc}.

Figure 5. In all cases acetonitrile was used as solvent. The nature of the voltammograms of the complexes under consideration do not change in dichloromethane. However, due to the relatively limited potential window of dichloromethane, acetonitrile was commonly used for voltammetric studies.

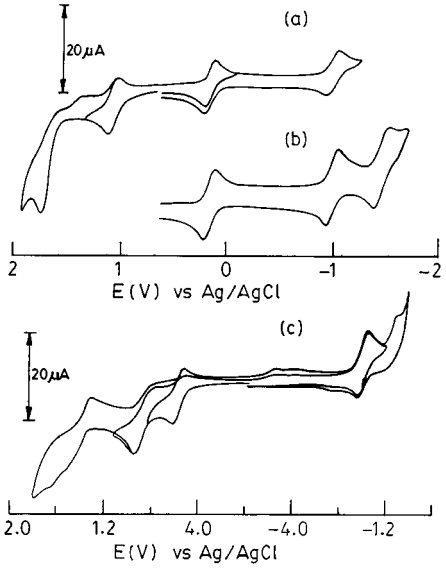

Figure 5. Cyclic voltammograms (scan rate 50 mVs^{-1}, solvent CH_3CN, 0.1 M TEAP) of (a) $[Fe(L^{2a})_2]ClO_4$ (platinum), (b) $[Fe(L^{2a})_2]ClO_4$ (glassy carbon), and (c) $Ni(L^{2a})_2$ (platinum)

The ferric complexes show four responses in the range +1.5 to −1.6 V. Three of these are cathodic, while the fourth one, occurring at ca. 1.0 V, is an anodic response. The free ligand $L^{2a}H$ displays[9] two irreversible anodic responses and a reversible cathodic response at 1.00, 1.30, and −1.15 V, respectively. The cathodic response in free $L^{2a}H$ is due to the reduction of the diazo function. For comparison, the parent ligand pap undergoes two successive step reductions at −1.31 and −1.57 V. Thus, the two cathodic responses in $\mathbf{1}^+$ at −0.97 and −1.45 V may be logically assigned to ligand reductions, centred mainly at the azoamide chromophore. The reductive response at +0.18 V and the oxidative response at 1.1 V both occur presumably at SOMO, which has almost equal metal and ligand contributions. These two responses may formally be assigned to Fe^{III}/Fe^{II} and Fe^{III}/Fe^{IV} couples. Presence of a hard donor site like $[ArN]^-$ in the deprotonated $[L^2]^-$ ligand helps in stabilisation of higher valent states of iron. For comparison, the ferrous state is highly stabilised in the parent $[Fe(pap)_3]^{2+}$ complex. The irreversible anodic response in $[\mathbf{1}]^+$ at > 1.7 V mainly concerns the oxidation of the amido function (SOMO-1).

Such low potentials for the Fe^{III}/Fe^{II} couple in $\mathbf{1}^+$ persuaded us to try and isolate the corresponding ferrous complex **1** in the pure state. Fortunately, with hydrazine as the reducing agent, we were able to isolate pink **1** in almost quantitative yield. This compound is thermally stable, but air-sensitive and is slowly reoxidised to $\mathbf{1}^+$ in the presence of air. In solution, the ferrous complex is a nonelectrolyte and is diamagnetic. Diamagnetism in this case confirms a low-spin state (t_2^6), which shows a highly resolved ^1H NMR spectrum. The nature of the ^1H NMR spectrum is similar to that observed for $[Co^{III}(L^2)_2]^+$.[6] The most notable feature in the infrared spectrum of **1a** is a large shift of $\nu_{N=N}$ to lower wavenumber (1300 cm^{-1}), indicating very strong $d_\pi - p_\pi$ interactions between the metal and ligand orbitals. For comparison, this vibration in the corresponding $[Fe(pap)_3]^{2+}$ complex is observed at 1350 cm^{-1}.[13] Our attempts to isolate the oxidized product, $[Fe(L^2)_2]^{2+}$ have so far been unsuccessful. Multiple electron-transfer responses are also the main features for the nickel complexes. These show two adjacent oxidative responses at ca. 0.56 and 0.85 V. The first one of these is reversible and the second one is only partly chemically reversible ($i_{pa} > i_{pc}$). Another high potential ligand-based irreversible oxidation process at > 1.4 V was also observed. The isolation of corresponding cationic $[\mathbf{2}]^+$ by chemical oxidation has been unsuccessful.

Spectroelectrochemistry

In order to study the spectra of the parent as well as other stable members of the redox series, two representative examples viz. $[Fe(L^{2a})_2]ClO_4$, $[\mathbf{1a}]ClO_4$, and $[Ni(L^{2a})_2]$ (**2a**) were chosen for spectroelectrochemical studies. These were performed in an OTTLE cell.[18] In both cases dichloromethane was used as solvent to take advantage of the higher solubilities of the complexes. The spectral data are collected in Table 2.

Figure 6 shows the solution spectra of the parent $\mathbf{1a}^+$ along with electrogenerated $\mathbf{1a}^{2+}$, **1a**, and $\mathbf{1a}^-$. The starting complex $\mathbf{1a}^+$ shows a very broad transition at 2125 nm (ε = 1070 $M^{-1}cm^{-1}$) in the NIR region. There are also two ill-defined shoulders at 1170 and 1055 nm. High-intensity multiple CT transitions ($\varepsilon \geq 10{,}000$ $M^{-1}cm^{-1}$) in the visible and UV range are the characteristics of all the above spectra. Upon oxidation, $\mathbf{1a}^+ \rightarrow \mathbf{1a}^{2+}$, the above broad NIR transition in $\mathbf{1a}^+$ is shifted to 2050 nm (ε = 2950 $M^{-1}cm^{-1}$), which is associated with a less-intense transition at 1635 nm (ε = 535 $M^{-1}cm^{-1}$). The intensities of NIR transitions for the present examples are too intense for a d−d transition. The lowest energy transition in $\mathbf{1a}^{2+}$ presumably involves two molecular orbitals that are ligand (SOMO-1, donor) and metal-ligand (SOMO, acceptor) orbitals. Hence, this transition is formally a ligand-to-metal charge-transfer (LMCT) transition. Notably, the corresponding Mn complex, $[Mn(L^{2a})_2]^+$, also shows[9] a similar transition at 2250 nm. The NIR region transitions in the case of **1a** appear at 1240 and 1440 nm. Upon further reduction to $\mathbf{1a}^-$, the NIR transitions completely disappear. The highly intense visible-range transitions may be due to SOMO→LUMO transitions. The rest of the high-energy transitions are assigned as intra-ligand transitions. It should be noted here that the free ligand $L^{2a}H$ shows[9] an intense transition at 490 nm, which is due to amido→azo charge transfer. All the above redox processes viz. $\mathbf{1a}^+ \rightleftarrows \mathbf{1a}^{2+}$, $\mathbf{1a}^+ \rightleftarrows \mathbf{1a}$ and $\mathbf{1a} \rightleftarrows \mathbf{1a}^-$ are reversible, and the spectrum of each of them

Table 2. Electronic spectral data

Compound	Absorption[a] λ_{max} [nm (ε [$M^{-1}cm^{-1}$])]
$[Fe(L^{2a})_2]ClO_4$	2125 (1070), 1170[b] (1610), 1055[b] (1600), 860[b] (6960), 760 (8300), 570[b] (9640), 510 (13120), 360[b] (17680)
$[Fe(L^{2a})_2]^{2+}$[c]	2050 (2950), 1635[b] (540), 860[b] (4280), 660[b] (9910), 610[b] (13120), 560[b] (13400), 380[b] (23800), 320[b] (20600)
$[Fe(L^{2a})_2]$[c]	1440[b] (1070), 1240[b] (1060), 820[b] (7230), 740(9640),670 (9100), 570(15260), 480[b] (10200), 340(19010), 300[b] (29200)
$[Fe(L^{2a})_2]^-$ [c]	770[b] (7770), 580(7770), 400(18750), 340[b] (19300)
$[Fe(L^{2b})_2]ClO_4$	760[b] (5900), 580[b] (6000), 510(9300), 420[b] (9540), 360[b] (13200)
$[Ni(L^{2a})_2]$	720[b] (20400), 680[b] (21340), 400(15380), 300[b] (28560), 250[b] (35460)
$[Ni(L^{2a})_2]^+$ [c]	1570[b] (1570), 1210[b] (1260), 700[b] (13200), 360 (19000), 260 (31400)
$[Ni(L^{2b})_2]$	730[b] (19500), 680[b] (17000), 400[b] (14300), 360[b] (12300), 250[b] (46900), 230 (51520)

[a] Data obtained from absorption spectra. – [b] Shoulder. – [c] Spectroelectrochemically generated compound in an OTTLE cell (see text).

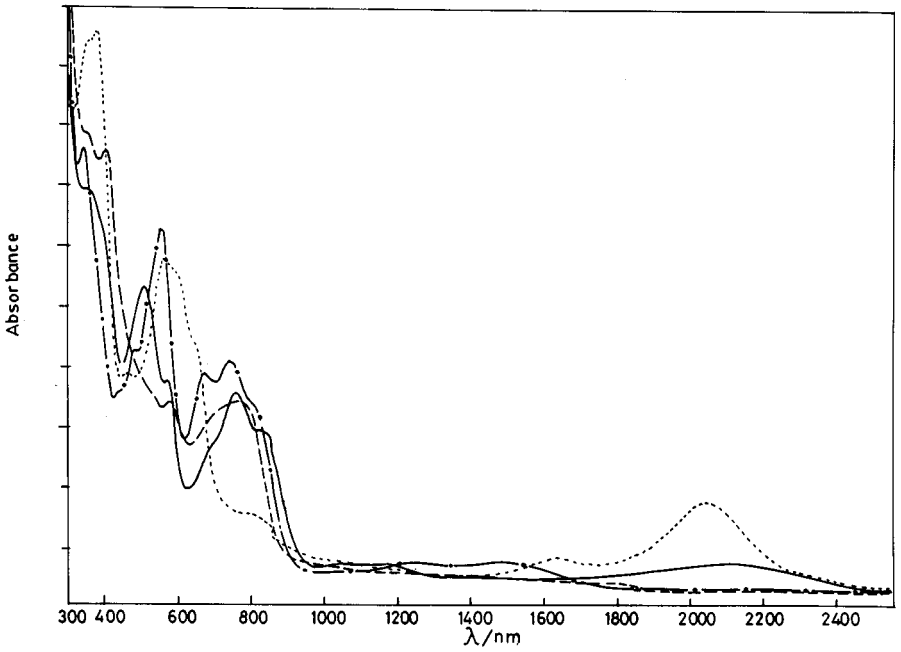

Figure 6. Solution spectra of $[Fe(L^{2a})_2]^+$ (—), $[Fe(L^{2a})_2]^{2+}$ (·····), $[Fe(L^{2a})_2]$ (– · – · –), and $[Fe(L^{2a})_2]^-$ (- - - - -).

may be quantitatively generated by application of the appropriate potential.

A spectroelectrochemical study on $[Ni(L^{2a})_2]$ (**2a**) was confined only to one reversible oxidation process, viz. **2a** $\rightleftarrows$ $\mathbf{2a}^+$ (see Supporting Information). The other redox processes are not chemically reversible, and these are not reported. Like the other transition metal complexes of this ligand system, the starting nickel(II) complex **2a** also shows multiple allowed CT transitions in the visible and UV region. Upon oxidation of the complex to $\mathbf{2a}^+$ the two low-energy transitions at 1570 and 1210 nm appear.

Conclusions

Metal-promoted amination of the pendant aromatic ring of a coordinated diazo ligand together with the chemistry of the transformed ligands involving iron and nickel are the two major aspects of this report. This work further demonstrates that, upon coordination, the ligand pap is susceptible to a fascinating metal-mediated chemical transformations. Earlier it was demonstrated that the pendant phenyl group of pap can be hydroxylated[4a] and thiolated[4b] by C–H activation. In the present study we have been able to isolate the aminated ligands that show interesting modifications of properties as ligands. The *ortho* fusion of the above type results in the formation of a potent N,N,N donor, which stabilises the rare low-spin state of both Fe^{III} and Fe^{II}. This anionic ligand has a unique combination of hard and soft donor sites. Extensive charge delocalisation plays a crucial role in the stabilization of low-spin state of the iron(III) complex. The study of coordination chemistry of both L^2H and L^3H involving heavier transition elements is in progress.

Experimental Section

Materials: The starting complexes $[Co(L^1)_3](ClO_4)_2$, $[Fe(L^1)_3](ClO_4)_2$, $[Ni(L^1)_3](ClO_4)_2$, and L^2H were prepared by reported

methods.[9,20] The solvents and chemicals used for synthesis were of analytical grade. The supporting electrolyte tetraethylammonium perchlorate (TEAP) and solvents for electrochemical work were obtained as before.[21]

Caution: Perchlorate salts of metal complexes were generally explosive. Although no detonation tendencies have been observed, care is advised and handling of only small quantities is recommended.

Physical Measurements: A Shimadzu UV 2100 UV/Vis spectrophotometer was used to record electronic spectra. − The IR spectra were recorded with a Perkin-Elmer 783 spectrophotometer. − ^{1}H NMR spectra in $CDCl_3$ were recorded with a Bruker Avance DPX300 spectrophotometer. $SiMe_4$ was used as an internal standard. − A Perkin−Elmer 240C elemental analyser was used to collect microanalytical data (C,H,N). − Electrochemical measurements were performed under dry nitrogen with an EG&G PARC Model 273A Potentiostat/Galvanostat based electrochemistry system. All potentials reported in this work are referenced to the Ag/AgCl electrode and are uncorrected for junction contribution. − The pH measurements were made with a μ-pH system 361 Systronics pH meter, standardised with buffers of pH = 7.0 and 9.2. − Electrical conductivities were measured by using a Systronics Direct Reading Conductivity meter 304. The pK_a values of the ligands were determined pH-metrically as described before.[21] − EPR measurements were made with a Varian 109C E-line X-band spectrometer fitted with a flat cell. Spectra were calibrated with the help of DPPH (g = 2.0037). − Magnetic moment measurements were carried out by using a PAR 155 vibrating sample magnetometer fitted with a Walker Scientific L75FBAL magnet. − Spectroelectrochemical studies were carried out in an OTTLE cell mounted in the sample compartment of a Perkin−Elmer Lambda 19 spectrophotometer, as described earlier.[18]

Isolation of 2-[4-(Arylamino)phenyl]azopyridine, L^3H: The reaction of neat $ArNH_2$ ($ArNH_2$ = aniline or *p*-toluidine) with $[Fe(L^1)_3](ClO_4)_2$ produced a blue mixture from which no pure product could be isolated. However, this crude product was used to isolate L^3H in the pure state. Details are given below. − The above crude product (0.10 g, $ArNH_2$ = aniline) was dissolved in methanol (30 mL) and NH_3(aq) (5 mL) was added. The mixture was then stirred for 30 min at a room temperature. The resulting yellow solution was concentrated to dryness under vacuum. The residue was then extracted with benzene and subjected to column chromatography on a silica gel (1 × 15 cm) column. A yellow band of $L^{3a}H$ was eluted with a benzene/chloroform mixture (3:1, v/v). The yellow extract was taken to dryness under vacuum. X-ray quality crystals were obtained at room temperature by slow diffusion of a benzene solution of the compound into hexane. Yield:0.06 g (60%). − UV/Vis (CH_2Cl_2): λ_{max} (ε, $M^{-1}cm^{-1}$) = 270 (10400), 415 (20800), 545(sh) nm. − IR (KBr): $\tilde{\nu}$ = 1575 (C=N), 1450 cm^{-1} (N=N). − ^{1}H NMR ($CDCl_3$): δ = 6.12 (s, N−H), 7.02 (d, J = 8.92 Hz, 2 H, 9-H and 11-H), 7.16 (4 H, 14-H,18-H and 15-H,17-H), 7.29 (t, J = 8.36 and 7.39 Hz, 1 H, 5-H), 7.72 (d, J = 8.0 Hz, 1 H, 3-H), 7.80 (t, J = 8.06 and 7.20 Hz, 1 H, 4-H), 7.93 (d, J = 8.86 Hz, 2 H, 8-H and 12-H), 8.64 (d, J = 4.73 Hz, 1 H, 6-H) (Figure 7). − pK_a = 9.1 ± 1. − $C_{17}H_{14}N_4$ (274.32): calcd. C 74.37, H 5.10, N 20.41; found C 74.02, H 5.63, N 20.04. − Similarly $L^{3b}H$ ($ArNH_2$ = *p*-toluidine) was isolated as orange needles following the above procedure. Yield: 58%. − UV/Vis (CH_2Cl_2): λ_{max} (ε, $M^{-1}cm^{-1}$) = 275 (11400), 410 (19000), 550(sh) nm. − IR (KBr): $\tilde{\nu}$ = 1595 (C=N), 1455 cm^{-1} (N=N). − ^{1}H NMR ($CDCl_3$): δ = 6.09 (s, N−H), 7.02 (d, J = 8.90 Hz, 2 H, 9-H and 11-H), 7.17 (4 H, 14-H,18-H and 15-H,17-H), 7.35 (t, J = 7.85 and 7.12 Hz, 1 H, 5-H), 7.79 (d, J = 7.94 Hz, 1 H, 3-H), 7.85 (t, J = 8.06 and 7.16 Hz, 1 H, 4-H), 7.97 (d, J = 8.85 Hz, 2 H, 8-H and 12-H), 8.70 (d, J = 3.67 Hz, 1 H, 6-H). − pK_a = 9.5 ± 1. − $C_{18}H_{16}N_4$ (288.32): calcd. C 74.92, H 5.55, N 19.42; found C 75.38, H 5.68, N 19.49.

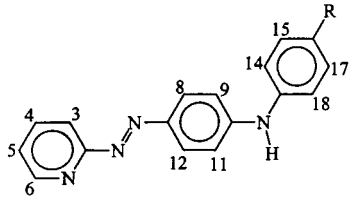

Figure 7. Numbering scheme for the protons of ligand L^3H

Synthesis of Bis[2-(2-phenylamido)phenyl)azopyridine]iron(III) Perchlorate, $[Fe(L^{2a})_2]ClO_4$, [1a]ClO_4: The ligand $L^{2a}H$ (0.11 g, 0.41 mmol) was dissolved in 25 mL of methanol and 1−2 drops of triethylamine were added. To this deprotonated ligand solution was added a methanolic solution of anhydrous $FeCl_3$ (0.03 g, 0.20 mmol) and the mixture was stirred for 1 h at a room temperature. The colour of the solution changed from orange yellow to reddish brown. The resulting solution was filtered and 5 mL of a dilute aqueous solution of $NaClO_4$ (ca. 1 M) was added. X-ray quality crystals were obtained at room temperature by slow diffusion of a dichloromethane solution of the compound into hexane. Yield: 0.12 g (85%). − IR (KBr): $\tilde{\nu}$ = 1595 (C=N), 1370 (N=N), 1100, 625 cm^{-1} (ClO_4^-). − Λ_M = 135 $\Omega^{-1}cm^2mol^{-1}$ (1 × 10^{-3} M in CH_3CN). − μ_{eff} (298 K) = 1.66 μ_B. − $C_{34}H_{26}ClFeN_8O_4$(701.93): calcd. C 58.13, H 3.70, N 15.96; found C 58.53, H 3.94, N 15.17. − Similarly, anhydrous $FeCl_3$ was treated with $L^{2b}H$ in a 1:2 ratio in methanolic solution in the presence of 1−2 drops of triethylamine as base. Subsequent addition of aqueous $NaClO_4$ to the reaction mixture produced crystalline $[Fe(L^{2b})_2]ClO_4$ (**1b**). Yield: 80%. − IR (KBr): $\tilde{\nu}$ = 1595 (C=N), 1365 (N=N), 1100, 625 cm^{-1} (ClO_4^-). − Λ_M = 140 Ω^{-1} cm^2mol^{-1} ($1{\cdot}10^{-3}$ M in CH_3CN). − μ_{eff} (298 K) = 1.68 μ_B. − $C_{36}H_{30}ClFeN_8O_4$ (729.93): calcd. C 59.18, H 4.11, N 15.34; found C 59.32, H 4.45, N 15.98.

Chemical Reduction of $[Fe^{III}(L^{2a})_2]ClO_4$ {[1a]ClO_4} to $[Fe^{II}(L^{2a})_2]$ {[1a]}: A dichloromethane solution of [**1a**]ClO_4 (0.10 g in 20 mL) was stirred with 5 mL of dilute aqueous hydrazine solution at room temperature for 30 min. The colour of the solution changed from reddish-brown to pink. The above mixture was extracted with dichloromethane (2 × 10 mL), which was then dried with anhydrous sodium sulfate. The dried solution was concentrated to half of its initial volume. Slow addition of hexane to the above pink solution precipitated dark microcrystals of **1a**. This was further crystallised from a dichloromethane/hexane solvent mixture. The compound is diamagnetic. Yield: 95%. − IR (KBr): $\tilde{\nu}$ = 1595 (C=N), 1300 cm^{-1} (N=N). − $C_{34}H_{26}FeN_8$ (602.43): calcd. C, 67.73, H 4.32, N 18.59; found C 67.46, H 4.73, N 18.30.

Synthesis of Bis[2-{2-(phenylamido)phenyl}azopyridine]nickel(II), $[Ni(L^{2a})_2]$, [2a]: The ligand $L^{2a}H$, (0.20 g, 0.74 mmol) was dissolved in 25 mL of methanol and 1−2 drops of triethylamine were added. To the deprotonated ligand solution was added a methanolic solution of $NiCl_2{\cdot}6H_2O$ (0.09 g, 0.37 mmol), and the mixture was stirred for 1 h at room temperature. The colour of the solution changed from orange yellow to green. The resultant mixture was filtered and the solvent was evaporated under vacuum. The compound thus obtained was finally crystallised from a dichlorome-

Table 3. Crystallographic data collection parameters for complexes

	[1a]ClO_4	2a	$L^{3a}H$
Empirical formula	$C_{34}H_{26}ClFeN_8O_4$	$C_{34}H_{26}N_8Ni$	$C_{17}H_{14}N_4$
Molecular mass	701.93	605.34	274.32
Temperature [K]	295(2)	295(2)	295(2)
Crystal system	triclinic	monoclinic	monoclinic
Space group	$P\bar{1}$	$P2_1/n$	$P2_1/c$
a [Å]	9.1859(1)	10.4656(12)	13.3331(6)
b [Å]	10.3559(1)	16.215(2)	9.8123(5)
c [Å]	17.2478(1)	16.821(2)	11.8449(5)
α [°]	103.887(1)	90	90
β [°]	91.143(1)	90.575(10)	114.595(1)
γ [°]	93.850(1)	90	90
V [Å^3]	1588.10(2)	2854.5(6)	1409.05(11)
Z	2	4	4
$D_{calcd.}$ [Mg/m^3]	1.468	1.409	1.293
Crystal dimensions [mm]	0.40 × 0.20 × 0.15	0.50 × 0.50 × 0.50	0.40 × 0.25 × 0.16
θ range for data collection [°]	1.22−26.37	1.74−25.00	1.68−25.00
GOF	1.001	1.033	1.048
Wavelength [Å]	0.71073	0.71073	0.71073
Reflections collected	18996	5037	6832
Unique reflections	6502	5037	2482
Largest difference between peak and hole [eÅ^{-3}]	0.364, −0.371	0.280, −0.274	0.162, −0.147
Final R indices [$I > 2\sigma(I)$]	$R1$ = 0.0370 $wR2$ = 0.1018	$R1$ = 0.0334 $wR2$ = 0.0783	$R1$ = 0.0469 $wR2$ = 0.0994

thane/hexane mixture. X-ray quality crystals were obtained at room temperature by slow diffusion of a dichloromethane solution of the compound into hexane. Yield: 0.19 g (85%). − IR (KBr): $\tilde{\nu}$ = 1595 (C=N), 1370 cm^{-1} (N=N). − μ_{eff} (298 K) = 2.89 μ_B. − $C_{34}H_{26}N_8Ni$ (605.34): calcd. C 67.40, H 4.30, N 18.50; found C 67.67, H 4.80, N 18.32. − Similarly, $NiCl_2{\cdot}6H_2O$ was treated with $L^{2b}H$ in a 1:2 ratio in methanolic solution in the presence of 1−2 drops of triethylamine as base to produce crystalline [Ni(L^{2b})$_2$] (**2b**). Yield: 80%. − IR (KBr): $\tilde{\nu}$ = 1595 (C=N), 1375 cm^{-1} (N=N). − μ_{eff} (298 K) = 2.92 μ_B. − $C_{36}H_{30}N_8Ni$ (633.34): C 68.21, H 4.74, N 17.68; found C 68.92, H 5.03, N 17.53.

Crystal Structure Determination: The crystallographic data for the compounds $L^{3a}H$, Fe(L^{2a})$_2ClO_4$, [**1a**]ClO_4, and Ni(L^{2a})$_2$ (**2a**) are collected in Table 3. The data were corrected for Lorentz and polarisation effects. All the structures were solved by using SHELXS-86 package of programme.[22] These revealed the positions of all non-hydrogen atoms and refined by full-matrix least-squares techniques against F^2 (SHELXL-93).[23] Absorption corrections were made with the SADABS package of programs. Hydrogen atoms were placed at the calculated positions. Crystallographic data (excluding structure factors) for the structures reported in this paper have been deposited with the Cambridge Crystallographic Data Centre as supplementary publication no. CCDC-141470, -141471, -141472. Copies of the data can be obtained free of charge on application to CCDC, 12 Union Road, Cambridge CB2 1EZ, UK [Fax: (internat.) + 44-1223/336-033; E-mail: deposit@ccdc.cam.ac.uk].

Acknowledgments

Financial support received from the Department of Science and Technology, New Delhi, is acknowledged. We are grateful to Professor J. A. McCleverty, Dr. M. D. Ward, University of Bristol, and Dr. S. Bhattacharya for their help. S. G. thanks the RSC for its financial support, which allowed him to visit the University of Bristol. We are thankful to the referees for suggestions.

[1] D. St. C. Black, *Comprehensive Coordination Chemistry* (Eds: R. D. Gillard, J. A. McCleverty), Pergamon Press, **1987**, vol. 1, p. 415; vol. 6, p. 155.
[2] L. S. Hegedus, *Coord. Chem. Rev.* **1998**, *168*, 49; L. S. Hegedus, *Coord. Chem. Rev.* **1998**, *175*, 159.
[3] K. N. Mitra, S.-M. Peng, S. Goswami, *Chem. Commun.* **1998**, 1685.
[4] [4a] P. Bandyopadhyay, D. Bandyopadhyay, A. Chakravorty, F. A. Cotton, L. R. Falvello, S. Han, *J. Am. Chem. Soc.* **1983**, *105*, 6327. − [4b] B. K. Santra, G. A. Thakur, P. Ghosh, A. Pramanik, G. K. Lahiri, *Inorg. Chem.* **1996**, *35*, 3050. − [4c] G. K. Lahiri, S. Goswami, L. R. Falvello, A. Chakravorty, *Inorg. Chem.* **1987**, *13*, 1714.
[5] [5a] J. F. Hartwig, *Angew. Chem. Int. Ed. Engl.* **1998**, *37*, 2046. − [5b] M. Bruncko, T.-A. V. Khoung, K. B. Sharpless, *Angew. Chem. Int. Ed. Engl.* **1996**, *35*, 454. − [5c] S. D. Gray, J. L. Thorman, V. A. Adamian, K. M. Kadish, K. L. Woo, *Inorg. Chem.* **1998**, *37*, 1. − [5d] Z. Li, R. W. Quan, E. N. Jacobsen, *J. Am. Chem. Soc.* **1995**, *117*, 5889.
[6] A. Saha, A. K. Ghosh, P. Majumdar, K. N. Mitra, S. Mondal, K. K. Rajak, L. R. Falvello, S. Goswami, *Organometallics* **1999**, *18*, 3772.
[7] A. K. Ghosh, P. Majumdar, L. R. Falvello, G. Mostafa, S. Goswami, *Organometallics* **1999**, *18*, 5086.
[8] [8a] S. Goswami, R. N. Mukherjee, A. Chakravorty, *Inorg. Chem.* **1983**, *22*, 2825. − [8b] B. K. Ghosh, A. Mukhopadhyay, S. Goswami, S. Ray, A. Chakravorty, *Inorg. Chem.* **1984**, *23*, 4633. − [8c] M. N. Ackermann, C. R. Barton, C. J. Deodene, E. M. Specht, S. C. Keill, W. E. Schreibet, M. Kim, *Inorg. Chem.* **1989**, *28*, 397.
[9] A. Saha, P. Majumdar, S. Goswami, *J. Chem. Soc., Dalton Trans.* **2000**, 1703.
[10] M. Ray, D. Ghosh, Z. Shirin, R. Mukherjee, *Inorg. Chem.* **1997**, *36*, 3568 and references therein.
[11] S. Karmakar, S. B. Choudhury, A. Chakravorty, *Inorg. Chem.* **1994**, *33*, 6148.
[12] [12a]S. Wolowiec, L. Latos-Grazynski, M. Mazzanti, J. C. Marchen, *Inorg. Chem.* **1997**, *36*, 5761. − [12b] C. Morice, P. L. Maux, G. Simonneaux, *Inorg. Chem.* **1998**, *37*, 6100.
[13] B. S. Raghavendra, A. Chakravorty, *Indian J. Chem., Sect. A* **1976**, *14A*, 166.
[14] P. Majumdar, S.-M. Peng, S. Goswami, *J. Chem. Soc., Dalton Trans.* **1998**, 1569.

[15] W. J. Greary, *Coord. Chem. Rev.* **1971**, *7*, 81.
[16] W. P. Griffith, *Coord. Chem. Rev.* **1975**, *17*, 177.
[17] C. Mealli, D. M. Proserpio, *J. Chem. Educ.* **1990**, *67*, 399.
[18] S.-M. Lee, M. Marcaccio, J. A. McCleverty, M. D. Ward, *Chem. Mater.* **1998**, *10*, 3272.
[19] A. K. Mahapatra, Ph. D. Thesis, Jadavpur University, India, **1989**.
[20] S. Choudhury, A. K. Deb, S. Goswami, *J. Chem. Soc., Dalton Trans.* **1994**, 1305.
[21] P. Ghosh, A. Chakravorty, *J. Chem. Soc., Dalton Trans.* **1985**, 361.
[22] G. M. Sheldrick, *SHELXS-86, Program for the solution of crystal structures*, University of Göttingen, **1990**.
[23] G. M. Sheldrick, *SHELXL-93, Program for the solution of crystal structures*, University of Göttingen, **1993**.

Received December 21, 1999
[I99464]